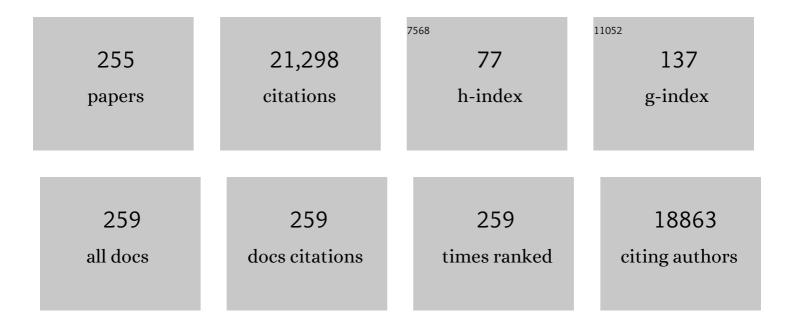
## Teik-Thye Lim

List of Publications by Year in descending order

Source: https://exaly.com/author-pdf/2579482/publications.pdf Version: 2024-02-01



TEIK-THVE LIM

#	Article	IF	CITATIONS
1	Generation of sulfate radical through heterogeneous catalysis for organic contaminants removal: Current development, challenges and prospects. Applied Catalysis B: Environmental, 2016, 194, 169-201.	20.2	1,966
2	Application of layered double hydroxides for removal of oxyanions: A review. Water Research, 2008, 42, 1343-1368.	11.3	1,423
3	Conversion of sewage sludge to clean solid fuel using hydrothermal carbonization: Hydrochar fuel characteristics and combustion behavior. Applied Energy, 2013, 111, 257-266.	10.1	727
4	Templateâ€free Formation of Uniform Urchinâ€like <i>α</i> â€FeOOH Hollow Spheres with Superior Capability for Water Treatment. Advanced Materials, 2012, 24, 1111-1116.	21.0	504
5	Graphene- and CNTs-based carbocatalysts in persulfates activation: Material design and catalytic mechanisms. Chemical Engineering Journal, 2018, 354, 941-976.	12.7	448
6	Enhancing sulfacetamide degradation by peroxymonosulfate activation with N-doped graphene produced through delicately-controlled nitrogen functionalization via tweaking thermal annealing processes. Applied Catalysis B: Environmental, 2018, 225, 243-257.	20.2	416
7	Evaluation of kapok (Ceiba pentandra (L.) Gaertn.) as a natural hollow hydrophobic–oleophilic fibrous sorbent for oil spill cleanup. Chemosphere, 2007, 66, 955-963.	8.2	344
8	Recent development of mixed metal oxide anodes for electrochemical oxidation of organic pollutants in water. Applied Catalysis A: General, 2014, 480, 58-78.	4.3	269
9	C–N–S tridoped TiO2 for photocatalytic degradation of tetracycline under visible-light irradiation. Applied Catalysis A: General, 2011, 399, 252-261.	4.3	267
10	Hierarchical TiO <sub>2</sub> Nanoflakes and Nanoparticles Hybrid Structure for Improved Photocatalytic Activity. Journal of Physical Chemistry C, 2012, 116, 2772-2780.	3.1	262
11	Design and application of heterogeneous catalysts as peroxydisulfate activator for organics removal: An overview. Chemical Engineering Journal, 2019, 358, 110-133.	12.7	248
12	Shear-strength characteristics of a residual soil. Canadian Geotechnical Journal, 1995, 32, 60-77.	2.8	244
13	Enhancing the catalytic activity of g-C 3 N 4 through Me doping (Me = Cu, Co and Fe) for selective sulfathiazole degradation via redox-based advanced oxidation process. Chemical Engineering Journal, 2017, 323, 260-269.	12.7	243
14	Solvothermal synthesis of C–N codoped TiO2 and photocatalytic evaluation for bisphenol A degradation using a visible-light irradiated LED photoreactor. Applied Catalysis B: Environmental, 2010, 100, 355-364.	20.2	236
15	Adsorption-photocatalytic degradation of Acid Red 88 by supported TiO2: Effect of activated carbon support and aqueous anions. Chemical Engineering Journal, 2011, 171, 1098-1107.	12.7	234
16	Geochemistry of inorganic arsenic and selenium in a tropical soil: effect of reaction time, pH, and competitive anions on arsenic and selenium adsorption. Chemosphere, 2004, 55, 849-859.	8.2	233
17	Removal of cytostatic drugs from aquatic environment: A review. Science of the Total Environment, 2013, 445-446, 281-298.	8.0	233
18	Enhanced photocatalytic degradation of bisphenol A with Ag-decorated S-doped g-C3N4 under solar irradiation: Performance and mechanistic studies. Chemical Engineering Journal, 2018, 333, 739-749.	12.7	209

#	Article	IF	CITATIONS
19	Hydrothermal gasification of sewage sludge and model compounds for renewable hydrogen production: A review. Renewable and Sustainable Energy Reviews, 2014, 39, 1127-1142.	16.4	207
20	Emergency water supply: A review of potential technologies and selection criteria. Water Research, 2012, 46, 3125-3151.	11.3	204
21	Fate and distribution of heavy metals during thermal processing of sewage sludge. Fuel, 2018, 226, 721-744.	6.4	203
22	Effect of rainfall on matric suctions in a residual soil slope. Canadian Geotechnical Journal, 1996, 33, 618-628.	2.8	202
23	Comparative evaluation of iodoacids removal by UV/persulfate and UV/H2O2 processes. Water Research, 2016, 102, 629-639.	11.3	202
24	Catalytic Reduction of Chlorobenzenes with Pd/Fe Nanoparticles:  Reactive Sites, Catalyst Stability, Particle Aging, and Regeneration. Environmental Science & Technology, 2007, 41, 7523-7529.	10.0	196
25	Surface–active bismuth ferrite as superior peroxymonosulfate activator for aqueous sulfamethoxazole removal: Performance, mechanism and quantification of sulfate radical. Journal of Hazardous Materials, 2017, 325, 71-81.	12.4	193
26	Ag–AgBr/TiO2/RGO nanocomposite for visible-light photocatalytic degradation of penicillin G. Journal of Materials Chemistry A, 2013, 1, 4718.	10.3	190
27	Zr-doped TiO2 for enhanced photocatalytic degradation of bisphenol A. Applied Catalysis A: General, 2010, 375, 107-115.	4.3	178
28	SERS-Encoded Nanogapped Plasmonic Nanoparticles: Growth of Metallic Nanoshell by Templating Redox-Active Polymer Brushes. Journal of the American Chemical Society, 2014, 136, 6838-6841.	13.7	174
29	A novel quasi-cubic CuFe <sub>2</sub> O <sub>4</sub> –Fe <sub>2</sub> O <sub>3</sub> catalyst prepared at low temperature for enhanced oxidation of bisphenol A via peroxymonosulfate activation. Journal of Materials Chemistry A, 2015, 3, 22208-22217.	10.3	169
30	Insights into the thermolytic transformation of lignocellulosic biomass waste to redox-active carbocatalyst: Durability of surface active sites. Applied Catalysis B: Environmental, 2018, 233, 120-129.	20.2	169
31	Enhanced Arsenic Removal by Hydrothermally Treated Nanocrystalline Mg/Al Layered Double Hydroxide with Nitrate Intercalation. Environmental Science & Technology, 2009, 43, 2537-2543.	10.0	168
32	Treatment of organics in reverse osmosis concentrate from a municipal wastewater reclamation plant: Feasibility test of advanced oxidation processes with/without pretreatment. Chemical Engineering Journal, 2011, 166, 932-939.	12.7	166
33	Carbonâ€Based Sorbents with Threeâ€Dimensional Architectures for Water Remediation. Small, 2015, 11, 3319-3336.	10.0	166
34	TiO <sub>2</sub> /AC Composites for Synergistic Adsorption-Photocatalysis Processes: Present Challenges and Further Developments for Water Treatment and Reclamation. Critical Reviews in Environmental Science and Technology, 2011, 41, 1173-1230.	12.8	164
35	Insights into nitrogen and boron-co-doped graphene toward high-performance peroxymonosulfate activation: Maneuverable N-B bonding configurations and oxidation pathways. Applied Catalysis B: Environmental, 2019, 253, 419-432.	20.2	163
36	Performance of magnetic activated carbon composite as peroxymonosulfate activator and regenerable adsorbent via sulfate radical-mediated oxidation processes. Journal of Hazardous Materials, 2015, 284, 1-9.	12.4	158

#	Article	IF	CITATIONS
37	Evaluation of hydrophobicity/oleophilicity of kapok and its performance in oily water filtration: Comparison of raw and solvent-treated fibers. Industrial Crops and Products, 2007, 26, 125-134.	5.2	155
38	Kinetic and mechanistic investigation of azathioprine degradation in water by UV, UV/H 2 O 2 and UV/persulfate. Chemical Engineering Journal, 2016, 302, 526-534.	12.7	153
39	Elucidation of stoichiometric efficiency, radical generation and transformation pathway during catalytic oxidation of sulfamethoxazole via peroxymonosulfate activation. Water Research, 2019, 151, 64-74.	11.3	148
40	Performance and mechanism of a hydrophobic–oleophilic kapok filter for oil/water separation. Desalination, 2006, 190, 295-307.	8.2	144
41	Photocatalytic degradation of bisphenol-A by nitrogen-doped TiO2 hollow sphere in a vis-LED photoreactor. Applied Catalysis B: Environmental, 2010, 95, 414-422.	20.2	143
42	Ag-decorated TiO2 photocatalytic membrane with hierarchical architecture: Photocatalytic and anti-bacterial activities. Water Research, 2014, 59, 207-218.	11.3	128
43	Carbon-sensitized and nitrogen-doped TiO2 for photocatalytic degradation of sulfanilamide under visible-light irradiation. Water Research, 2011, 45, 5015-5026.	11.3	126
44	Pathways and kinetics of carbon tetrachloride and chloroform reductions by nano-scale Fe and Fe/Ni particles: comparison with commercial micro-scale Fe and Zn. Chemosphere, 2005, 59, 1267-1277.	8.2	122
45	High surface area DPA-hematite for efficient detoxification of bisphenol A via peroxymonosulfate activation. Journal of Materials Chemistry A, 2014, 2, 15836-15845.	10.3	122
46	Urea-assisted one-step synthesis of cobalt ferrite impregnated ceramic membrane for sulfamethoxazole degradation via peroxymonosulfate activation. Chemical Engineering Journal, 2018, 343, 737-747.	12.7	119
47	Comparison of amoxicillin photodegradation in the UV/H2O2 and UV/persulfate systems: Reaction kinetics, degradation pathways, and antibacterial activity. Chemical Engineering Journal, 2019, 372, 420-428.	12.7	115
48	Superabsorbent Cryogels Decorated with Silver Nanoparticles as a Novel Water Technology for Point-of-Use Disinfection. Environmental Science & Technology, 2013, 47, 9363-9371.	10.0	113
49	Characteristics of incineration ash for sustainable treatment and reutilization. Environmental Science and Pollution Research, 2019, 26, 16974-16997.	5.3	113
50	Chemical recycling of plastic waste for sustainable material management: A prospective review on catalysts and processes. Renewable and Sustainable Energy Reviews, 2022, 154, 111866.	16.4	110
51	Low-temperature synthesis of graphene/Bi2Fe4O9 composite for synergistic adsorption-photocatalytic degradation of hydrophobic pollutant under solar irradiation. Chemical Engineering Journal, 2015, 262, 1022-1032.	12.7	106
52	Reductive dechlorination of 1,2,4-trichlorobenzene with palladized nanoscale FeO particles supported on chitosan and silica. Chemosphere, 2006, 65, 1137-1145.	8.2	104
53	A novel three-dimensional spherical CuBi <sub>2</sub> O <sub>4</sub> consisting of nanocolumn arrays with persulfate and peroxymonosulfate activation functionalities for 1H-benzotriazole removal. Nanoscale, 2015, 7, 8149-8158.	5.6	104
54	Processing of flexible plastic packaging waste into pyrolysis oil and multi-walled carbon nanotubes for electrocatalytic oxygen reduction. Journal of Hazardous Materials, 2020, 387, 121256.	12.4	103

#	Article	IF	CITATIONS
55	Influences of co-existing species on the sorption of toxic oxyanions from aqueous solution by nanocrystalline Mg/Al layered double hydroxide. Journal of Hazardous Materials, 2010, 180, 401-408.	12.4	100
56	Facile room-temperature synthesis of carboxylated graphene oxide-copper sulfide nanocomposite with high photodegradation and disinfection activities under solar light irradiation. Scientific Reports, 2015, 5, 16369.	3.3	100
57	Influences of Amphiphiles on Dechlorination of a Trichlorobenzene by Nanoscale Pd/Fe: Adsorption, Reaction Kinetics, and Interfacial Interactions. Environmental Science & Technology, 2008, 42, 4513-4519.	10.0	98
58	Catalytic hydrodechlorination of chlorophenols by Pd/Fe nanoparticles: Comparisons with other bimetallic systems, kinetics and mechanism. Separation and Purification Technology, 2010, 76, 206-214.	7.9	96
59	Synergistic catalytic degradation of antibiotic sulfamethazine in a heterogeneous sonophotolytic goethite/oxalate Fenton-like system. Applied Catalysis B: Environmental, 2013, 136-137, 294-301.	20.2	96
60	Facile synthesis of pure g-C3N4 materials for peroxymonosulfate activation to degrade bisphenol A: Effects of precursors and annealing ambience on catalytic oxidation. Chemical Engineering Journal, 2020, 387, 123726.	12.7	95
61	Pore-functionalized ceramic membrane with isotropically impregnated cobalt oxide for sulfamethoxazole degradation and membrane fouling elimination: Synergistic effect between catalytic oxidation and membrane separation. Applied Catalysis B: Environmental, 2019, 254, 37-46.	20.2	94
62	Process evaluation for optimization of EDTA use and recovery for heavy metal removal from a contaminated soil. Chemosphere, 2005, 58, 1031-1040.	8.2	91
63	Highly stable heterostructured Ag–AgBr/TiO2 composite: a bifunctional visible-light active photocatalyst for destruction of ibuprofen and bacteria. Journal of Materials Chemistry, 2012, 22, 23149.	6.7	91
64	Effects of sewage sludge organic and inorganic constituents on the properties of pyrolysis products. Energy Conversion and Management, 2019, 196, 1410-1419.	9.2	89
65	Chelating-Agent-Enhanced Heavy Metal Extraction from a Contaminated Acidic Soil. Journal of Environmental Engineering, ASCE, 2004, 130, 59-66.	1.4	88
66	Washing enhanced electrokinetic remediation for removal cadmium from real contaminated soil. Journal of Hazardous Materials, 2005, 123, 165-175.	12.4	86
67	Insights into the speciation of heavy metals during pyrolysis of industrial sludge. Science of the Total Environment, 2019, 691, 232-242.	8.0	86
68	Environmental impact assessment of converting flexible packaging plastic waste to pyrolysis oil and multi-walled carbon nanotubes. Journal of Hazardous Materials, 2020, 390, 121449.	12.4	86
69	Aging characteristics and reactivity of two types of nanoscale zero-valent iron particles (FeBH and) Tj ETQq1 1 0	.784314 r 12.7	gBT_{0verloc
70	Rapid degradation of sulfonamides in a novel heterogeneous sonophotochemical magnetite-catalyzed Fenton-like (US/UV/Fe3O4/oxalate) system. Applied Catalysis B: Environmental, 2014, 160-161, 325-334.	20.2	85
71	Arsenic fractionation in a fine soil fraction and influence of various anions on its mobility in the subsurface environment. Applied Geochemistry, 2005, 20, 229-239.	3.0	84
72	Effect of aqueous matrix species on synergistic removal of bisphenol-A under solar irradiation using nitrogen-doped TiO2/AC composite. Applied Catalysis B: Environmental, 2011, 101, 709-717.	20.2	84

#	Article	IF	CITATIONS
73	Preparation of carbon-sensitized and Fe–Er codoped TiO2 with response surface methodology for bisphenol A photocatalytic degradation under visible-light irradiation. Applied Catalysis B: Environmental, 2012, 126, 121-133.	20.2	83
74	Sorption characteristics and mechanisms of oxyanions and oxyhalides having different molecular properties on Mg/Al layered double hydroxide nanoparticles. Journal of Hazardous Materials, 2010, 179, 818-827.	12.4	82
75	Catalytically active nitrogen-doped porous carbon derived from biowastes for organics removal via peroxymonosulfate activation. Chemical Engineering Journal, 2019, 374, 947-957.	12.7	82
76	Surface-nucleated heterogeneous growth of zeolitic imidazolate framework – A unique precursor towards catalytic ceramic membranes: Synthesis, characterization and organics degradation. Chemical Engineering Journal, 2018, 353, 69-79.	12.7	81
77	Application of sequential extraction analysis to electrokinetic remediation of cadmium, nickel and zinc from contaminated soils. Journal of Hazardous Materials, 2010, 184, 547-554.	12.4	80
78	Highly efficient and stable Ag–AgBr/TiO2 composites for destruction of Escherichia coli under visible light irradiation. Water Research, 2013, 47, 4148-4158.	11.3	80
79	In-situ stabilization of Pb, Zn, Cu, Cd and Ni in the multi-contaminated sediments with ferrihydrite and apatite composite additives. Journal of Hazardous Materials, 2009, 170, 1093-1100.	12.4	79
80	Electrochemical treatment of olive mill wastewater. Journal of Chemical Technology and Biotechnology, 2007, 82, 663-671.	3.2	77
81	Bactericidal Mechanisms Revealed for Rapid Water Disinfection by Superabsorbent Cryogels Decorated with Silver Nanoparticles. Environmental Science & Technology, 2015, 49, 2310-2318.	10.0	77
82	Chelating agent-assisted electrokinetic removal of cadmium, lead and copper from contaminated soils. Environmental Pollution, 2009, 157, 3379-3386.	7.5	76
83	Products evolution during hydrothermal conversion of dewatered sewage sludge in sub- and near-critical water: Effects of reaction conditions and calcium oxide additive. International Journal of Hydrogen Energy, 2015, 40, 5776-5787.	7.1	76
84	A hot syngas purification system integrated with downdraft gasification of municipal solid waste. Applied Energy, 2019, 237, 227-240.	10.1	76
85	Kinetic modeling and energy efficiency of UV/H2O2 treatment of iodinated trihalomethanes. Water Research, 2015, 75, 259-269.	11.3	74
86	Synthesis and characterization of nitrogen-doped TiO2/AC composite for the adsorption–photocatalytic degradation of aqueous bisphenol-A using solar light. Catalysis Today, 2010, 151, 8-13.	4.4	73
87	Photodegradation of iodinated trihalomethanes in aqueous solution by UV 254 irradiation. Water Research, 2014, 49, 275-285.	11.3	73
88	Electrochemical oxidation of stabilized landfill leachate on DSA electrodes. Journal of Hazardous Materials, 2011, 190, 460-465.	12.4	71
89	Effect of hexamethylenetetramine on the visible-light photocatalytic activity of C–N codoped TiO2 for bisphenol A degradation: evaluation of photocatalytic mechanism and solution toxicity. Applied Catalysis A: General, 2011, 399, 233-241.	4.3	67
90	Chelate Agents Enhanced Electrokinetic Remediation for Removal Cadmium and Zinc by Conditioning Catholyte pH. Water, Air, and Soil Pollution, 2006, 172, 295-312.	2.4	66

#	Article	IF	CITATIONS
91	Assessment of the use of spent copper slag for land reclamation. Waste Management and Research, 2006, 24, 67-73.	3.9	66
92	A high-performance UV/visible photodetector of Cu <sub>2</sub> O/ZnO hybrid nanofilms on SWNT-based flexible conducting substrates. Journal of Materials Chemistry C, 2014, 2, 9536-9542.	5.5	66
93	Surface construction of nitrogen-doped chitosan-derived carbon nanosheets with hierarchically porous structure for enhanced sulfacetamide degradation via peroxymonosulfate activation: Maneuverable porosity and active sites. Chemical Engineering Journal, 2020, 382, 122908.	12.7	65
94	High-permeability pluronic-based TiO2 hybrid photocatalytic membrane with hierarchical porosity: Fabrication, characterizations and performances. Chemical Engineering Journal, 2013, 228, 1030-1039.	12.7	64
95	Conversion of non-condensable pyrolysis gases from plastics into carbon nanomaterials: Effects of feedstock and temperature. Journal of Analytical and Applied Pyrolysis, 2017, 124, 16-24.	5.5	64
96	Effects of anions on the kinetics and reactivity of nanoscale Pd/Fe in trichlorobenzene dechlorination. Chemosphere, 2008, 73, 1471-1477.	8.2	62
97	Nonradical transformation of sulfamethoxazole by carbon nanotube activated peroxydisulfate: Kinetics, mechanism and product toxicity. Chemical Engineering Journal, 2019, 378, 122147.	12.7	62
98	Hybrid catalytic ozonation-membrane filtration process with CeOx and MnOx impregnated catalytic ceramic membranes for micropollutants degradation. Chemical Engineering Journal, 2019, 378, 121670.	12.7	62
99	Sonophotolytic degradation of azo dye reactive black 5 in an ultrasound/UV/ferric system and the roles of different organic ligands. Water Research, 2011, 45, 2915-2924.	11.3	61
100	Experimental study on visible-light induced photocatalytic oxidation of gaseous formaldehyde by polyester fiber supported photocatalysts. Chemical Engineering Journal, 2013, 218, 9-18.	12.7	59
101	A facile synthesis of monodispersed hierarchical layered double hydroxide on silica spheres for efficient removal of pharmaceuticals from water. Journal of Materials Chemistry A, 2013, 1, 3877.	10.3	59
102	Upgrading of non-condensable pyrolysis gas from mixed plastics through catalytic decomposition and dechlorination. Fuel Processing Technology, 2018, 170, 13-20.	7.2	59
103	Pyrolysis derived char from municipal and industrial sludge: Impact of organic decomposition and inorganic accumulation on the fuel characteristics of char. Waste Management, 2019, 83, 131-141.	7.4	59
104	Solar regeneration of powdered activated carbon impregnated with visible-light responsive photocatalyst: Factors affecting performances and predictive model. Water Research, 2012, 46, 3054-3064.	11.3	58
105	In situ grown metallic nickel from X–Ni (X=La, Mg, Sr) oxides for converting plastics into carbon nanotubes: Influence of metal–support interaction. Journal of Cleaner Production, 2020, 258, 120633.	9.3	58
106	Solvothermal synthesis of Fe–C codoped TiO2 nanoparticles for visible-light photocatalytic removal of emerging organic contaminants in water. Applied Catalysis A: General, 2011, 409-410, 257-266.	4.3	57
107	In situ oil/water separation using hydrophobic–oleophilic fibrous wall: A lab-scale feasibility study for groundwater cleanup. Journal of Hazardous Materials, 2006, 137, 820-826.	12.4	56
108	Enhanced activation of peroxydisulfate by CuO decorated on hexagonal boron nitride for bisphenol A removal. Chemical Engineering Journal, 2020, 393, 124714.	12.7	55

#	Article	IF	CITATIONS
109	Poisoning effects of H2S and HCl on the naphthalene steam reforming and water-gas shift activities of Ni and Fe catalysts. Fuel, 2019, 241, 1008-1018.	6.4	54
110	Contamination Time Effect on Lead and Cadmium Fractionation in a Tropical Coastal Clay. Journal of Environmental Quality, 2002, 31, 806.	2.0	53
111	Multi-heteroatom-doped carbocatalyst as peroxymonosulfate and peroxydisulfate activator for water purification: A critical review. Journal of Hazardous Materials, 2022, 426, 128077.	12.4	53
112	Simultaneous degradation of 4CP and EDTA in a heterogeneous Ultrasound/Fenton like system at ambient circumstance. Separation and Purification Technology, 2009, 68, 367-374.	7.9	52
113	Design and synthesis of ice-templated PSA cryogels for water purification: towards tailored morphology and properties. Soft Matter, 2013, 9, 224-234.	2.7	51
114	Single-crystalline Bi <sub>2</sub> Fe <sub>4</sub> O <sub>9</sub> synthesized by low-temperature co-precipitation: performance as photo- and Fenton catalysts. RSC Advances, 2014, 4, 27820-27829.	3.6	51
115	Asymmetric TiO2 hybrid photocatalytic ceramic membrane with porosity gradient: Effect of structure directing agent on the resulting membranes architecture and performances. Ceramics International, 2014, 40, 6747-6757.	4.8	51
116	Rational design of hierarchically-structured CuBi <sub>2</sub> O <sub>4</sub> composites by deliberate manipulation of the nucleation and growth kinetics of CuBi <sub>2</sub> O <sub>4</sub> for environmental applications. Nanoscale, 2016, 8, 2046-2054.	5.6	51
117	A comparative study on electrochemical oxidation of bisphenol A by boron-doped diamond anode and modified SnO2-Sb anodes: Influencing parameters and reaction pathways. Journal of Environmental Chemical Engineering, 2016, 4, 2807-2815.	6.7	50
118	Degradation of cyclophosphamide and 5-fluorouracil in water using UV and UV/H 2 O 2 : Kinetics investigation, pathways and energetic analysis. Journal of Environmental Chemical Engineering, 2017, 5, 1133-1139.	6.7	49
119	Evaluation of the effect of dosage, pH and contact time on high-dose phosphate inhibition for copper corrosion control using response surface methodology (RSM). Corrosion Science, 2008, 50, 918-927.	6.6	48
120	Direct and indirect photodegradation pathways of cytostatic drugs under UV germicidal irradiation: Process kinetics and influences of water matrix species and oxidant dosing. Journal of Hazardous Materials, 2017, 324, 481-488.	12.4	46
121	Thermodynamic analyses of synthetic natural gas production via municipal solid waste gasification, high-temperature water electrolysis and methanation. Energy Conversion and Management, 2019, 202, 112160.	9.2	46
122	Acetic acid-assisted fabrication of hierarchical flower-like Bi2O3 for photocatalytic degradation of sulfamethoxazole and rhodamine B under solar irradiation. Journal of Colloid and Interface Science, 2017, 505, 489-499.	9.4	45
123	Evaluation of a submerged membrane vis-LED photoreactor (sMPR) for carbamazepine degradation and TiO2 separation. Chemical Engineering Journal, 2013, 215-216, 240-251.	12.7	44
124	Hierarchically-structured Co–CuBi 2 O 4 and Cu–CuBi 2 O 4 for sulfanilamide removal via peroxymonosulfate activation. Catalysis Today, 2017, 280, 2-7.	4.4	44
125	Kinetic and mechanistic examinations of reductive transformation pathways of brominated methanes with nano-scale Fe and Ni/Fe particles. Water Research, 2007, 41, 875-883.	11.3	43
126	Ultrafast Synthesis of Layered Titanate Microspherulite Particles by Electrochemical Spark Discharge Spallation. Chemistry - A European Journal, 2010, 16, 7704-7708.	3.3	43

#	Article	IF	CITATIONS
127	Cuboid-like Bi <sub>2</sub> Fe <sub>4</sub> O <sub>9</sub> /Ag with Graphene-Wrapping Tribrid Composite with Superior Capability for Environmental Decontamination: Nanoscaled Material Design and Visible-Light-Driven Multifunctional Catalyst. ACS Sustainable Chemistry and Engineering, 2015, 3, 2726-2736.	6.7	43
128	The role and fate of EDTA in ultrasound-enhanced zero-valent iron/air system. Chemosphere, 2010, 78, 576-582.	8.2	42
129	Nitrogen-doped TiO2/AC bi-functional composite prepared by two-stage calcination for enhanced synergistic removal of hydrophobic pollutant using solar irradiation. Catalysis Today, 2011, 161, 46-52.	4.4	41
130	Preparation, characterization and performance of a novel visible light responsive spherical activated carbon-supported and Er3+:YFeO3-doped TiO2 photocatalyst. Journal of Hazardous Materials, 2012, 199-200, 301-308.	12.4	40
131	Iron-mediated reduction rates and pathways of halogenated methanes with nanoscale Pd/Fe: Analysis of linear free energy relationship. Chemosphere, 2007, 66, 1765-1774.	8.2	39
132	Membrane vis-LED photoreactor for simultaneous penicillin G degradation and TiO2 separation. Water Research, 2012, 46, 1825-1837.	11.3	39
133	Polyacrylonitrile (PAN)-induced carbon membrane with in-situ encapsulated cobalt crystal for hybrid peroxymonosulfate oxidation-filtration process: Preparation, characterization and performance evaluation. Chemical Engineering Journal, 2019, 373, 425-436.	12.7	39
134	Evaluation of the cycling performance of a sorbent for H2S removal and simulation of desulfurization-regeneration processes. Chemical Engineering Journal, 2017, 326, 1255-1265.	12.7	38
135	High performance duplex-structured SnO2-Sb-CNT composite anode for bisphenol A removal. Separation and Purification Technology, 2017, 179, 25-35.	7.9	37
136	Reduction of chlorinated methanes with nano-scale Fe particles: Effects of amphiphiles on the dechlorination reaction and two-parameter regression for kinetic prediction. Chemosphere, 2008, 73, 1817-1823.	8.2	36
137	Enhanced electrochemical oxidation of phenol using a hydrophobic TiO <sub>2</sub> -NTs/SnO <sub>2</sub> -Sb-PTFE electrode prepared by pulse electrodeposition. RSC Advances, 2015, 5, 32245-32255.	3.6	36
138	Ultra-effective integrated technologies for water disinfection with a novel 0D-2D-3D nanostructured rGO-AgNP/Bi2Fe4O9 composite. Applied Catalysis B: Environmental, 2018, 227, 548-556.	20.2	36
139	Ni-Zn-based nanocomposite loaded on cordierite mullite ceramic for syngas desulfurization: Performance evaluation and regeneration studies. Chemical Engineering Journal, 2018, 351, 230-239.	12.7	36
140	Bimodal N-doped P25-TiO2/AC composite: Preparation, characterization, physical stability, and synergistic adsorptive-solar photocatalytic removal of sulfamethazine. Applied Catalysis A: General, 2012, 427-428, 125-136.	4.3	35
141	Influence of surface morphology on the performance of nanostructured ZnO-loaded ceramic honeycomb for syngas desulfurization. Fuel, 2018, 211, 591-599.	6.4	35
142	Contamination Time Effect on Lead and Cadmium Fractionation in a Tropical Coastal Clay. Journal of Environmental Quality, 2002, 31, 806-812.	2.0	34
143	Ordered mesoporous Zn-based supported sorbent synthesized by a new method for high-efficiency desulfurization of hot coal gas. Chemical Engineering Journal, 2018, 353, 273-287.	12.7	33
144	High-sulfur capacity and regenerable Zn-based sorbents derived from layered double hydroxide for hot coal gas desulfurization. Journal of Hazardous Materials, 2018, 360, 391-401.	12.4	33

Τεικ-Τηγε Lim

#	Article	IF	CITATIONS
145	A surfactant-thermal method to prepare crystalline thioantimonate for high-performance lithium-ion batteries. Inorganic Chemistry Frontiers, 2016, 3, 111-116.	6.0	32
146	Catalytic processing of non-condensable pyrolysis gas from plastics: Effects of calcium supports on nickel-catalyzed decomposition of hydrocarbons and HCl sorption. Chemical Engineering Science, 2018, 189, 311-319.	3.8	32
147	Microwave effects on the structure of CeO2-doped zinc oxide sorbents for H2S removal. Fuel, 2015, 146, 56-59.	6.4	31
148	Catalytic activities and resistance to HCl poisoning of Ni-based catalysts during steam reforming of naphthalene. Applied Catalysis A: General, 2018, 557, 25-38.	4.3	29
149	Barium aluminate improved iron ore for the chemical looping combustion of syngas. Applied Energy, 2020, 272, 115236.	10.1	29
150	Analytical assessment of tar generated during gasification of municipal solid waste: Distribution of GC–MS detectable tar compounds, undetectable tar residues and inorganic impurities. Fuel, 2020, 268, 117348.	6.4	29
151	Consolidation of cement-treated sewage sludge using vertical drains. Canadian Geotechnical Journal, 2005, 42, 528-540.	2.8	27
152	Preparation of graphene-MoS2 hybrid aerogels as multifunctional sorbents for water remediation. Science China Materials, 2017, 60, 1102-1108.	6.3	27
153	Distribution and modeling of tar compounds produced during downdraft gasification of municipal solid waste. Renewable Energy, 2019, 136, 1294-1303.	8.9	27
154	A comprehensive performance evaluation of heterogeneous Bi2Fe4O9/peroxymonosulfate system for sulfamethoxazole degradation. Environmental Science and Pollution Research, 2019, 26, 1026-1035.	5.3	27
155	Syntheses, crystal structures, and photocatalytic properties of two ammonium-directed Ag–Sb–S complexes. Inorganic Chemistry Frontiers, 2017, 4, 954-959.	6.0	26
156	Spatial confinement of cobalt crystals in carbon nanofibers with oxygen vacancies as a high-efficiency catalyst for organics degradation. Chemosphere, 2020, 245, 125407.	8.2	26
157	Ba–Al-decorated iron ore as bifunctional oxygen carrier and HCl sorbent for chemical looping combustion of syngas. Combustion and Flame, 2021, 223, 230-242.	5.2	26
158	Transformation behaviors and environmental risk assessment of heavy metals during resource recovery from Sedum plumbizincicola via hydrothermal liquefaction. Journal of Hazardous Materials, 2021, 410, 124588.	12.4	26
159	Flexible packaging plastic waste – environmental implications, management solutions, and the way forward. Current Opinion in Chemical Engineering, 2021, 32, 100684.	7.8	26
160	Effect of synthesis routes on the properties and bactericidal activity of cryogels incorporated with silver nanoparticles. RSC Advances, 2015, 5, 44626-44635.	3.6	25
161	UV direct photolysis of halogenated disinfection byproducts: Experimental study and QSAR modeling. Chemosphere, 2019, 235, 719-725.	8.2	25
162	Mesoporous Zn-Fe-based binary metal oxide sorbent with sheet-shaped morphology: Synthesis and application for highly efficient desulfurization of hot coal gas. Chemical Engineering Journal, 2020, 389, 123750.	12.7	25

#	Article	IF	CITATIONS
163	Musselâ€Inspired Dualâ€Superlyophobic Biomass Membranes for Selective Oil/Water Separation. Advanced Materials Interfaces, 2020, 7, 1901756.	3.7	25
164	Technical and environmental assessment of laboratory scale approach for sustainable management of marine plastic litter. Journal of Hazardous Materials, 2022, 421, 126717.	12.4	25
165	Forecasting quantities of critical raw materials in obsolete feature and smart phones in Greece: A path to circular economy. Journal of Environmental Management, 2022, 307, 114566.	7.8	25
166	Hydrostratigraphy and geochemistry at a coastal sandfill in Singapore. Hydrogeology Journal, 2007, 15, 1591-1604.	2.1	24
167	Degradation of chlorophenols (CPs) in an ultrasound-irradiated Fenton-like system at ambient circumstance: The QSPR (quantitative structure–property relationship) study. Chemical Engineering Journal, 2010, 156, 347-352.	12.7	24
168	Removal of arsenate from aqueous solution by nanocrystalline Mg/Al layered double hydroxide: sorption characteristics, prospects, and challenges. Water Science and Technology, 2010, 61, 1411-1417.	2.5	24
169	Insights into the single and binary adsorption of copper(II) and nickel(II) on hexagonal boron nitride: Performance and mechanistic studies. Journal of Environmental Chemical Engineering, 2019, 7, 102872.	6.7	24
170	High temperature slagging gasification of municipal solid waste with biomass charcoal as a greener auxiliary fuel. Journal of Hazardous Materials, 2022, 423, 127057.	12.4	24
171	Effects of cement on redistribution of trace metals and dissolution of organics in sewage sludge and its inorganic waste-amended products. Waste Management, 2006, 26, 1294-1304.	7.4	23
172	Effect of microwave irradiation on the preparation of iron oxide/arenaceous clay sorbent for hot coal gas desulfurization. Fuel Processing Technology, 2016, 148, 35-42.	7.2	23
173	Hot Coal Gas Desulfurization Using Regenerable ZnO/MCM41 Prepared via One-Step Hydrothermal Synthesis. Energy & Fuels, 2017, 31, 9814-9823.	5.1	23
174	Weakening the strong Fe-La interaction in A-site-deficient perovskite via Ni substitution to promote the thermocatalytic synthesis of carbon nanotubes from plastics. Journal of Hazardous Materials, 2021, 403, 123642.	12.4	23
175	Ce/TiOx-functionalized catalytic ceramic membrane for hybrid catalytic ozonation-membrane filtration process: Fabrication, characterization and performance evaluation. Chemical Engineering Journal, 2021, 410, 128307.	12.7	23
176	Chemical looping combustion-adsorption of HCl-containing syngas using alkaline-earth coated iron ore composites for simultaneous purification and combustion enhancement. Chemical Engineering Journal, 2021, 417, 129226.	12.7	23
177	Use of Fluorescein as a Ground Water Tracer in Brackish Water Aquifers. Ground Water, 2007, 45, 85-88.	1.3	22
178	Magnetically recyclable Bi/Fe-based hierarchical nanostructures via self-assembly for environmental decontamination. Nanoscale, 2016, 8, 12736-12746.	5.6	22
179	Sorption and Speciation of Heavy Metals from Incinerator Fly Ash in a Marine Clay. Journal of Environmental Engineering, ASCE, 1997, 123, 1107-1115.	1.4	21
180	Desulfurization of Hot Coal Gas over Regenerable Low-Cost Fe <sub>2</sub> O <sub>3</sub> /Mesoporous Al <sub>2</sub> O <sub>3</sub> Prepared by the Sol–Gel Method. Energy & Fuels, 2017, 31, 13921-13932.	5.1	21

#	Article	IF	CITATIONS
181	A Novel Metal–Organic Framework (MOF)–Mediated Interfacial Polymerization for Direct Deposition of Polyamide Layer on Ceramic Substrates for Nanofiltration. Advanced Materials Interfaces, 2019, 6, 1900132.	3.7	21
182	Polyoxometalates for bifunctional applications: Catalytic dye degradation and anticancer activity. Chemosphere, 2022, 286, 131869.	8.2	21
183	Selenium extractability from a contaminated fine soil fraction: implication on soil cleanup. Chemosphere, 2005, 58, 91-101.	8.2	20
184	New Way of Removing Hydrogen Sulfide at a High Temperature: Microwave Desulfurization Using an Iron-Based Sorbent Supported on Active Coke. Energy & Fuels, 2017, 31, 4263-4272.	5.1	20
185	Controllable mullite bismuth ferrite micro/nanostructures with multifarious catalytic activities for switchable/hybrid catalytic degradation processes. Journal of Colloid and Interface Science, 2018, 509, 502-514.	9.4	20
186	A novel real-time monitoring and control system for waste-to-energy gasification process employing differential temperature profiling of a downdraft gasifier. Journal of Environmental Management, 2019, 234, 65-74.	7.8	20
187	Regenerable Co-ZnO-based nanocomposites for high-temperature syngas desulfurization. Fuel Processing Technology, 2020, 201, 106344.	7.2	20
188	Universal and Switchable Omni-Repellency of Liquid-Infused Surfaces for On-Demand Separation of Multiphase Liquid Mixtures. ACS Nano, 2021, 15, 6977-6986.	14.6	20
189	Changes in mobility and speciation of heavy metals in clay-amended incinerator fly ash. Environmental Geology, 2004, 47, 1-10.	1.2	19
190	Nanostructured hexahedron of bismuth ferrite clusters: delicate synthesis processes and an efficient multiplex catalyst for organic pollutant degradation. RSC Advances, 2015, 5, 86891-86900.	3.6	19
191	Nickel-based catalysts for steam reforming of naphthalene utilizing gasification slag from municipal solid waste as a support. Fuel, 2019, 254, 115561.	6.4	19
192	Transport of cadmium and assessment of phytotoxicity after electrokinetic remediation. Journal of Environmental Management, 2008, 86, 535-544.	7.8	18
193	Iron ore modified with alkaline earth metals for the chemical looping combustion of municipal solid waste derived syngas. Journal of Cleaner Production, 2021, 282, 124467.	9.3	18
194	Thermodynamic analyses of a standalone diesel-fueled distributed power generation system based on solid oxide fuel cells. Applied Energy, 2022, 308, 118396.	10.1	18
195	Photoacoustic induced surface acoustic wave sensor for concurrent opto-mechanical microfluidic sensing of dyes and plasmonic nanoparticles. RSC Advances, 2016, 6, 50238-50244.	3.6	17
196	Real time size-dependent particle segregation and quantitative detection in a surface acoustic wave-photoacoustic integrated microfluidic system. Sensors and Actuators B: Chemical, 2017, 252, 568-576.	7.8	17
197	One-step construction of heterostructured metal-organics@Bi2O3 with improved photoinduced charge transfer and enhanced activity in photocatalytic degradation of sulfamethoxazole under solar light irradiation. Chemosphere, 2018, 205, 396-403.	8.2	17
198	Effective H2S control during chemical looping combustion by iron ore modified with alkaline earth metal oxides. Energy, 2021, 218, 119548.	8.8	17

#	Article	IF	CITATIONS
199	Impact of vertical electrokinetic-flushing technology to remove heavy metals and polycyclic aromatic hydrocarbons from contaminated soil. Electrochimica Acta, 2012, 86, 72-79.	5.2	16
200	Potential evaluation and perspectives on using sponge-like superabsorbent cryogels for onsite water treatment in emergencies. Desalination and Water Treatment, 2015, 53, 1506-1515.	1.0	16
201	Hierarchical Graphene/Metal–Organic Framework Composites with Tailored Wettability for Separation of Immiscible Liquids. ACS Applied Materials & Interfaces, 2020, 12, 35563-35571.	8.0	16
202	One-Step Block Copolymer Templated Synthesis of Bismuth Oxybromide for Bisphenol A Degradation: An Extended Study from Photocatalysis to Chemical Oxidation. ACS ES&T Water, 2021, 1, 837-846.	4.6	16
203	Insights into the synergistic role of catalytic ceramic membranes for ozone and peroxymonosulfate activation towards effective recalcitrant micropollutant degradation and mineralization. Chemical Engineering Journal, 2022, 430, 132921.	12.7	16
204	In Situ Preparation and Regeneration Behaviors of Zinc Oxide/Red Clay Desulfurization Sorbents. Energy & Fuels, 2017, 31, 1015-1022.	5.1	15
205	Advanced Ni tar reforming catalysts resistant to syngas impurities: Current knowledge, research gaps and future prospects. Fuel, 2022, 318, 123602.	6.4	15
206	A novel molybdenum-based nanocrystal decorated ceramic membrane for organics degradation via catalytic wet air oxidation (CWAO) at ambient conditions. Catalysis Today, 2021, 364, 276-284.	4.4	14
207	Dual-functional witherite in improving chemical looping performance of iron ore and simultaneous adsorption of HCl in syngas at high temperature. Chemical Engineering Journal, 2021, 413, 127538.	12.7	14
208	Tailoring Fe2O3–Al2O3 catalyst structure and activity via hydrothermal synthesis for carbon nanotubes and hydrogen production from polyolefin plastics. Chemosphere, 2022, 297, 134148.	8.2	14
209	Unexpected Intrinsic Catalytic Function of Porous Boron Nitride Nanorods for Highly Efficient Peroxymonosulfate Activation in Water Treatment. ACS Applied Materials & Interfaces, 2022, 14, 18409-18419.	8.0	14
210	Structure Characteristics and Hot-Coal-Gas Desulfurization Properties of Zn-Based Sorbents Supported on Mesoporous Silica with Different Pore-Arrangement Patterns: A Comparison Study. Energy & Fuels, 2021, 35, 2456-2467.	5.1	12
211	Insights into the effects of metal-ion doping on the structure and hot-coal-gas desulfurization properties of Zn-based sorbents supported on SBA-15. Fuel, 2022, 315, 123198.	6.4	12
212	Insights to the microwave effect in the preparation of sorbent for H2S removal: Desulfurization kinetics and characterization. Fuel, 2017, 203, 233-243.	6.4	11
213	Fe-Based Sorbent for Hot Coal Gas under Microwave Irradiation: Desulfurization Performance and Microwave Effects. Energy & Fuels, 2019, 33, 9004-9013.	5.1	11
214	Modulating local environment of Ni with W for synthesis of carbon nanotubes and hydrogen from plastics. Journal of Cleaner Production, 2022, 352, 131620.	9.3	11
215	Catalysing electrowinning of copper from E-waste: A critical review. Chemosphere, 2022, 298, 134340.	8.2	11
216	Highly efficient activation of peroxymonosulfate by bismuth oxybromide for sulfamethoxazole degradation under ambient conditions: Synthesis, performance, kinetics and mechanisms. Separation and Purification Technology, 2021, 276, 119203.	7.9	10

#	Article	IF	CITATIONS
217	Hydrogen bromide in syngas: Effects on tar reforming, water gas-shift activities and sintering of Ni-based catalysts. Applied Catalysis B: Environmental, 2021, 280, 119435.	20.2	9
218	Impact of solution chemistry on the properties and bactericidal activity of silver nanoparticles decorated on superabsorbent cryogels. Journal of Colloid and Interface Science, 2016, 461, 104-113.	9.4	8
219	Dynamic estimation of future obsolete laptop flows and embedded critical raw materials: The case study of Greece. Waste Management, 2021, 132, 74-85.	7.4	8
220	Thermal behavior of Cu-Mg-Al-Ba/Sr bifunctional composites during chemical looping combustion and HCl adsorption of MSW syngas. Chemical Engineering Journal, 2022, 430, 132871.	12.7	8
221	Temperature-dependent synthesis of multi-walled carbon nanotubes and hydrogen from plastic waste over A-site-deficient perovskite La0.8Ni1-xCoxO3-δ. Chemosphere, 2022, 291, 132831.	8.2	8
222	Characterization of an acoustically coupled multilayered microfluidic platform on SAW substrate using mixing phenomena. Sensors and Actuators A: Physical, 2015, 233, 360-367.	4.1	7
223	Highly active and poison-tolerant nickel catalysts for tar reforming synthesized through controlled hydrothermal synthesis. Applied Catalysis A: General, 2020, 607, 117779.	4.3	7
224	Concomitant Electro-Fenton Processes in Iron-Based Electrocoagulation Systems for Sulfanilamide Degradation: Roles of Ca <sup>2+</sup> in Fe(II)/Fe(III) Complexation and Electron Transfer. ACS ES&T Water, 2022, 2, 778-785.	4.6	7
225	Influence of Metal Loading on the Mode of Metal Retention in a Natural Clay. Journal of Environmental Engineering, ASCE, 2001, 127, 539-545.	1.4	6
226	Speciation of heavy metals in surface sediments from Suzhou Creek. Journal of Shanghai University, 2007, 11, 415-425.	0.1	6
227	Pyrolysis kinetics of ZnAl LDHs and its calcined products for H2S removal. Journal of Thermal Analysis and Calorimetry, 2018, 132, 581-589.	3.6	6
228	A facile energy-saving and environmental oil-spill remedial method: Separation patterns and kinetics research. Applied Surface Science, 2021, 556, 149761.	6.1	6
229	Controlled field studies on soil aquifer treatment in a constructed coastal sandfill. Water Science and Technology, 2009, 60, 1283-1293.	2.5	5
230	Effective surface treatment techniques for refinishing oil-stained road surface. Construction and Building Materials, 2018, 159, 64-72.	7.2	5
231	Recent Biotechnology Advances in Bio-Conversion of Lignin to Lipids by Bacterial Cultures. Frontiers in Chemistry, 2022, 10, 894593.	3.6	5
232	Polydopamineâ€Mediated Superlyophobic Polysiloxane Coating of Porous Substrates for Efficient Separation of Immiscible Liquids. Advanced Materials Interfaces, 2020, 7, 2000428.	3.7	4
233	Higher bacterial diversity in two-phase thermophilic anaerobic digestion of food waste after micronutrient supplementation. Biomass Conversion and Biorefinery, 2023, 13, 5187-5195.	4.6	4
234	Modeling the Life Cycle Inventory of a Centralized Composting Facility in Greece. Applied Sciences (Switzerland), 2022, 12, 2047.	2.5	4

Τεικ-Τηγε Lim

#	Article	IF	CITATIONS
235	Significance of Aqueous Cation Composition on Heavy Metal Mobility in a Natural Clay. Water Environment Research, 2002, 74, 346-353.	2.7	3
236	Mechanistic and thermodynamic studies of oxyanion sorption by various synthetic Mg/Al layered double hydroxides. Water Science and Technology, 2009, 59, 1011-1017.	2.5	3
237	The Effects of Washing Techniques on Thermal Combustion Properties of Sewage Sludge Chars. International Journal of Environmental Research, 2021, 15, 285-297.	2.3	3
238	Unravelling the significance of catalyst reduction stage for high tar reforming activity in the presence of syngas impurities. Applied Catalysis A: General, 2022, 642, 118711.	4.3	3
239	Use of Sewage Sludge and Copper Slag for Land Reclamation. , 2008, , .		2
240	Practical Applications of Bimetallic Nanoiron Particles for Reductive Dehalogenation of Haloorganics: Prospects and Challenges. ACS Symposium Series, 2010, , 245-261.	0.5	2
241	DOC and UVA attenuation with soil aquifer treatment in the saturated zone of an artificial coastal sandfill. Water Science and Technology, 2010, 62, 491-500.	2.5	2
242	A molybdovanadophosphate-based surfactant encapsulated heteropolyanion with multi-lamellar nano-structure for catalytic wet air oxidation of organic pollutants under ambient conditions. RSC Advances, 2015, 5, 94743-94751.	3.6	2
243	Preparation of mesoporous MCMâ€41 supported zinc sorbents by microwave inâ€situ oxidation for H 2 S removal in coal gas. Canadian Journal of Chemical Engineering, 2020, 98, 1729-1740.	1.7	2
244	CHAPTER 5. Combined Photocatalysis–Separation Processes for Water Treatment Using Hybrid Photocatalytic Membrane Reactors. RSC Energy and Environment Series, 2016, , 130-156.	0.5	2
245	FEM modelling of a SAW microfluidic sensor based on the photoacoustic effect. , 2016, , .		1
246	Selective leaching of scandium and yttrium from red mud induced by hydrothermal treatment. Journal of Chemical Technology and Biotechnology, 2021, 96, 2620-2629.	3.2	1
247	Mixed-addenda polyoxometalates for enhanced electrochemical water oxidation. MRS Advances, 2021, 6, 588-593.	0.9	1
248	EXPERIMENTAL EVALUATION OF A NATURAL HOLLOW HYDROPHOBIC-OLEOPHILIC FIBER FOR ITS POTENTIAL APPLICATION IN NAPL SPILL CLEANUP1. International Oil Spill Conference Proceedings, 2005, 2005, 815-818.	0.1	1
249	Photodegradation of Cytostatic Drugs in Low-Pressure UV Photoreactor Through Direct and Indirect Pathways. , 2020, , 245-257.		1
250	Geochemical changes during recharge with tertiary-treated wastewater at a coastal sandfill. Water Science and Technology, 2009, 60, 1273-1281.	2.5	0
251	Treatment of RO Concentrate for Enhanced Water Recovery from Wastewater Treatment Plant Effluent. Handbook of Environmental Chemistry, 2014, , 247-268.	0.4	0

0

#	Article	IF	CITATIONS
253	Carbon: Carbonâ€Based Sorbents with Threeâ€Dimensional Architectures for Water Remediation (Small) Tj ETQ	q110784 10.0784	4314 rgBT /○\
254	Nanostructured Catalytic and Adsorbent Materials for Water Remediation. , 2016, , 75-111.		0
255	Synthesis and Characterization of Nano-scale Clay Anion Exchanger and Its Application in Removing Arsenic from Aqueous System. Journal of Ion Exchange, 2007, 18, 316-321.	0.3	Ο